



ELSEVIER

Thermochimica Acta 284 (1996) 47–56

thermochimica
acta

Thermal fractionation of ethylene polymers in packaging applications¹

Mimi Keating^{a,*}, I-Hwa Lee^a, Chun Sing Wong^b

^a *E.I. duPont de Nemours & Company, Wilmington, DE 19880, USA*

^b *DuPont Canada Inc., Kingston, Canada, K7L 5A5*

Abstract

In the past 5 years, new ethylene copolymers have found their way into a wide variety of applications. The new polymers have a unique combination of properties not typically found in conventional elastomeric or thermoplastic ethylene polymers. The characterization of these polymers by new and improved analytical techniques is of great interest. We describe a thermal fractionation method which sorts the crystalline ethylene sequence lengths of the polymer into groups. The ethylene lengths are estimated using melting points of known hydrocarbons. Three statistical terms are introduced to describe ethylene sequence length distribution: the arithmetic mean \bar{L}_n , the weighted mean L_w and the broadness index L_w/\bar{L}_n . We demonstrate the technique by comparing ethylene polymers produced with different catalyst systems, decipher ethylene components in unidentified ethylene blends and track changes in crystalline fractions with grafting.

Keywords: Adhesives; Ethylene copolymers; Grafting; Stepwise recrystallization; Thermal fractionation

1. Introduction

The introduction of linear very low density polyethylene (VLDPE) and ultra low density polyethylene (ULDPE), a family of polyethylenes (PE) that bridges the density gap between linear low density polyethylene (LLDPE) of 0.915 g/ml^{-1} to ethylene

* Corresponding author.

¹ Presented at the 24th North American Thermal Analysis Society Conference, San Francisco, CA, U.S.A., 10–13 September 1995

propylene rubber (EPR) of 0.87 g ml^{-1} , offers the packaging industry new materials. These PEs show a unique combination of properties not typically found in conventional elastomeric or thermoplastic ethylene polymers, namely, flexibility, high resilience toughness, and heat and puncture resistance. Used alone or in blends with LLDPE, HDPE or ethylene-co-vinyl acetate (EVA), these PEs can expand their temperature range of applications in food, industrial and medical packaging, in adhesives, in wire and cable, and as impact modifiers. A survey of the literature and patents shows applications in wraps, shrink bags, liners, hospital gloves, tubings and transdermal drug delivery devices, frozen food packagers, agricultural tunnels, greenhouse covers, coextrudable adhesives and peelable seal for snacks.

The characterization of VLDPEs and ULDPEs by new and improved analytical techniques is of great interest. A recent review of temperature rising elution fractionation (TREF), a chromatographical separation method introduced in 1982 by Wild et al. [1], demonstrates its renewed practical use [2–3]. Bonner et al. [4] show a calibration for TREF. Mathot and Pijpers [5] show intermolecular heterogeneity of comonomer incorporation in VLDPE by TREF and SSF, and conclude that comonomers are excluded from the crystal lattice based on the heat capacity values of a two-phase model. Following treatment by TREF [6–7] and high-pressure crystallization at 5 kbar [7], a heterogeneous morphology of VLDPE and LLDPE were determined using DSC melting and TEM. Other reports include correlation of melt instability and shear-history-dependent rheology [8], high dielectric loss spectra of gamma-irradiated LLDPE [9], and high shear viscosity, low elongational viscosity and melt fracture at low shear rate in LLDPE [10]. A thermal fractionation method [11] used in our lab is the preferred technique to compare comonomer distribution based on stepwise recrystallization of ethylene segments between the branch points. The crystals are melt-crystallized according to a sequentially decreasing temperature program, rather than being solution grown as in the TREF technique.

2. Materials

We selected a variety of commercial polyethylene (Table 1) and ethylene-polymer-based adhesives (in Table 2) to demonstrate the flexibility and range of this fractionation technique.

3. Results and discussion

The family of VLDPE, ULDPE and LLDPE available to the packaging industry varies in the method of manufacture, the type and level of comonomer, and the molecular weight distribution (MWD). The major physical properties are controlled by these parameters. Producers use above-conventional amounts of α -olefin comonomer to drive the density down. We believe that finer-scale properties, such as clarity, sealability and processability, are associated with the heterogeneity of comonomer distribution along the polymer chain. The “heterogeneity” is often shown as branch

Table 1
Commercial polyethylenes studied

Grade	Manufacturer	MI ^a 190°C dg min ⁻¹	Density/ g cm ⁻³	Melt peak/ °C	Comonomer type	Comonomer % ^b	MWD ^c
Flexomer 9042	Union Carbide	5.1	0.901	122	1-Butene	15.5	4.8
Flexomer 1085	Union Carbide	0.8	0.884	116	1-Butene	23.5	5.3
Exact 3028	Exxon	1.2	0.901	94	1-Butene	10.8	1.8
Attane 4201	Dow	1.0	0.912	123	1-Octene	12.9	
Ultzex 2022 L	Mitsui		0.920	124	4-Methyl- 1-pentene	8.8	

^a Melt index.

^b By ¹³C NMR.

^c Molecular weight distribution, by gel permeation chromatography.

Table 2
Commercial ethylene-polymer- based adhesives studied

Adhesive ^a	MI190°C dg min ^{-1b}	Density/g cm ⁻³	Melt point/°C	Vicat/°C ^c	% Maleic anhydride ^d
ADH-1	4.5	0.90	123, 68	58	0.05
ADH-2	1.0	0.91	123, 106	90	0.37
ADH-3	4.6	0.92	125, 95	100	0.12
ADH-4	11.4	N/A	98	N/A	0.04

^a Adhesive grades obtained from 3 different companies.

^b Melt index. ^c ASTM test. ^d Measured by IR.

content difference by TREF and multiple melting peaks by DSC. Thermal fractionation is a clean and clear-cut way [11] to estimate the ethylene run sequence between the branch points with a calibration of hydrocarbon standards. This information is useful to identify the source of ethylene in a blend.

3.1. Thermal fractionation

Thermal fractionation is a temperature-dependent segregation process based on recrystallization and reorganization of ethylene chains from the melt. It is similar to TREF, but the segregation mode is different. The neighboring sequences can crystallize independently and subsequently melt at temperatures corresponding to their crystal size or lamellar thickness. Large intramolecular sequence heterogeneity results in more levels of segregation. Because there is no actual physical separation of the macromolecules, intra- and intermolecular heterogeneity are equally assessed. We simply take a snap-shot at the fractions after the fractionation.

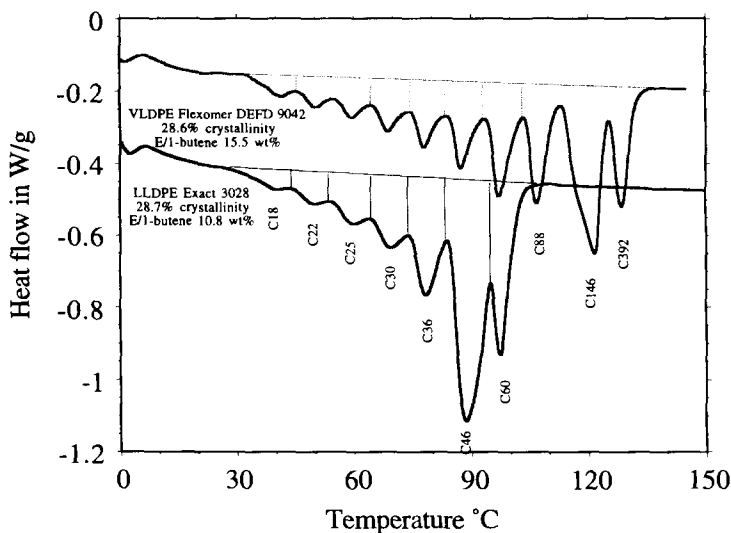


Fig. 1. Narrow versus broad comonomer distribution of two ethylene/1-butene polymers with identical crystallinity and density: Flexomer DEFD 9042 (top curve) and Exact 3028 (bottom curve).

In Fig. 1, the profiles of thermally fractionated Flexomer DEFD 9042 and Exact 3028 are compared. The two are very different: the former is a Unipol[®]-based random copolymer with a broad MWD and the latter is an Exxpol[®] metallocene-based copolymer with a narrow MWD. The comonomer distributions of the two copolymers are reflected in a collection of ethylene run lengths, which have no relation to MWD. Flexomer 9042 exhibits a broad distribution from short ($T_m = 40^\circ\text{C}$) to very long ($T_m = 130^\circ\text{C}$) ethylene runs, whereas Exact 3028 shows a relatively narrow distribution from short ($T_m = 40^\circ\text{C}$) to medium ($T_m = 100^\circ\text{C}$) run length.

During fractionation, as the molten polymer is held at the highest crystallization temperature, the longest ethylene sequence solidifies by chain folding, a preferable configuration to interchain aggregation due to its lower end surface energy [12]. The segregation by sequence length can reach equilibrium, since a 12-h reorganization time is allowed. Segregation of the next longest group follows as the temperature decreases by 10°C . The long spacing between the lamellar stacks measured by time-resolved Small-Angle X-Ray Scattering (SAXS) as a function of temperature supports this segregation theory. For Exact 3028, the long spacing is in the order of 240 \AA when crystallized at 80°C and down to 100 \AA when crystallized at 40°C [13]. Once the crystalline network is laid out by crystals of long ethylene sequences, the short sequences between the long runs will solidify by chain folding or aggregation as lamellar fillers and may not be grouped by the exact length. The error is relatively small at the low temperature end, since the melting point becomes less sensitive to length, as discussed below.

3.2. Calibration

To estimate the sequence length, we recrystallized the commercially available hydrocarbons with the same program and measured the subsequent melting points. We included HDPE. The plot of $\ln(\text{CH}_2 \text{ mole fraction})$ against $1/T/^\circ\text{K}$ is shown in Fig. 2. From this curve, the ethylene sequence length of fractionated ethylene copolymers can be assigned from the melting temperatures of the fractions. For example, in Fig. 1, the crystallizable sequences of Flexomer 9042 range from $(\text{CH}_2)_{18}$ to the longest of $(\text{CH}_2)_{393}$. Exact 3028, however, shows sequences from $(\text{CH}_2)_{18}$ to only $(\text{CH}_2)_{60}$.

Similar numerical expressions for molecular weight distribution based on moments [14] can be used here to describe the ethylene sequence distribution. We introduce the terms of “arithmetic mean \bar{L}_n ” of the sequence length L distribution

$$\bar{L}_n = \frac{n_1 L_1 + n_2 L_2 + \dots + n_j L_j}{n_1 + n_2 + \dots + n_j} = \frac{n_1}{N} L_1 + \frac{n_2}{N} L_2 + \dots + \frac{n_j}{N} L_j = \sum f_i L_i$$

the weighted mean \bar{L}_w of the sequence length L distribution

$$\bar{L}_w = \frac{n_1 L_1^2 + n_2 L_2^2 + \dots + n_j L_j^2}{n_1 L_1 + n_2 L_2 + \dots + n_j L_j} = \frac{\sum f_i L_i^2}{\sum f_i L_i}$$

and the broadness index, \bar{L}_w/\bar{L}_n .

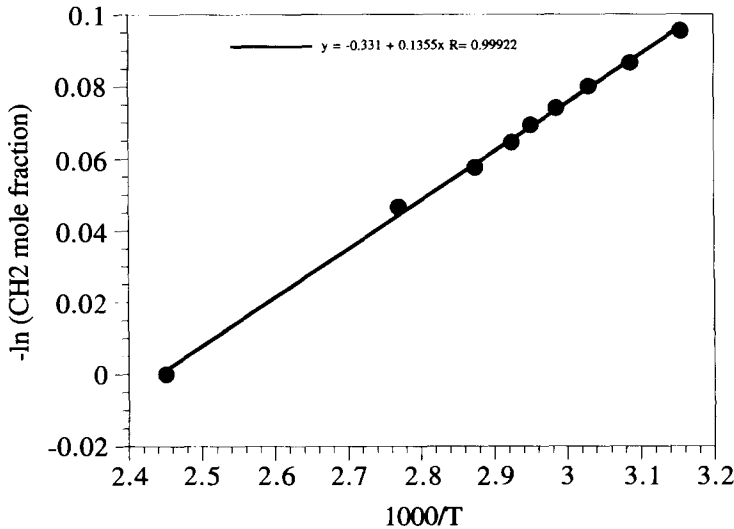


Fig. 2. Sequence length calibration based on melting points of known hydrocarbons.

3.3. Comonomer type

We compared Flexomer 1085, Attane 4201 and Ultzex 2022 L from three different product lines which use 1-butene, 1-octene and 4-methyl-1-pentene, respectively, as the comonomer source. All three products were made with conventional catalysts and possess broad comonomer distribution. We did not expect the comonomer type to make a difference in fractionation, since large side groups of ethyl, hexyl and isobutyl will be excluded from the crystalline phase. All were treated as branch points.

In Fig. 3, the broadness indices $\overline{L_w}/\overline{L_n}$ of the three are similar in the range of 1.84–1.89, but the $\overline{L_n}$, $\overline{L_w}$ and crystallinity are different. Ultzex 2022 L has the least amount of comonomer of 8.8 wt% 4-methyl-1-pentene, the highest crystallinity of 44.2%, and the highest average ethylene repeating units, $\overline{L_n} = 73.0$, $\overline{L_w} = 134.5$, $\overline{L_w}/\overline{L_n} = 1.84$. Attane 4201 has 12.9 wt% 1-octene, 40.4% crystallinity, and average ethylene repeating units at $\overline{L_n} = 56.9$, $\overline{L_w} = 107.3$, $\overline{L_w}/\overline{L_n} = 1.89$. Flexomer 1085 has the largest amount of comonomer of 23.5 wt% 1-butene, the lowest crystallinity of 15.6%, and shortest average ethylene repeating units at $\overline{L_n} = 35.6$, $\overline{L_w} = 67.0$, $\overline{L_w}/\overline{L_n} = 1.88$. Since the calibration is in semi-logarithmic scale, the highest melting peak is much more sensitive to the sequence length than the lowest melting peaks: 50 methylene units per 1°C versus 3 units per 10°C. At the high end, 0.9°C drop in melting point corresponds to a difference of 44 methylene units: $T_m = 129.5^\circ\text{C}$ for $(\text{CH}_2)_{364}$ and $T_m = 128.6^\circ\text{C}$ for $(\text{CH}_2)_{320}$. In the slightly lower range, it takes a 3.1°C decrease to shorten the sequence length by 23 methylene units: $T_m = 120.0^\circ\text{C}$ for $(\text{CH}_2)_{145}$ and

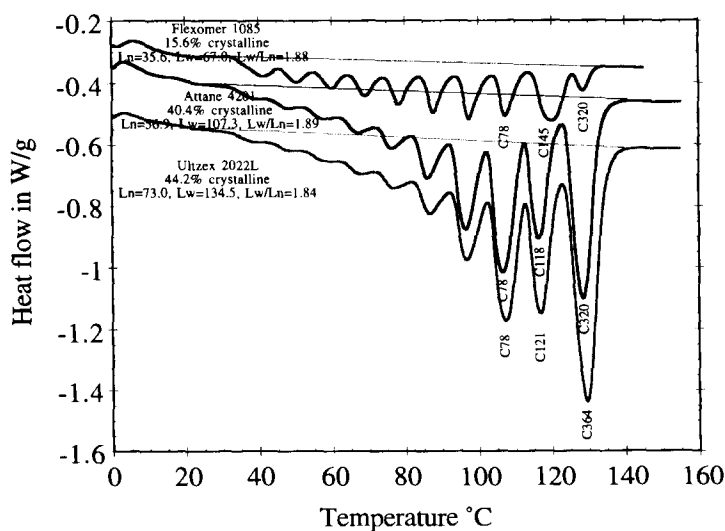


Fig. 3. Three broad ethylene copolymers in a range of crystallinity and sequence distribution: Flexomer 1085 (top curve), Attane 4201 (middle) and Ultzex 2022 L (bottom).

$T_m = 116.9^\circ\text{C}$ for $(\text{CH}_2)_{121}$. At still lower range, a 9.2°C decrease shortens the sequence by 40 methylene units: $T_m = 116.4^\circ\text{C}$ for $(\text{CH}_2)_{118}$, $T_m = 107.2^\circ\text{C}$ for $(\text{CH}_2)_{78}$.

3.4. Adhesives

Thermal fractionation has proven to be an invaluable tool for elucidating the components of unidentified blends, when used in conjunction with other analytical techniques, such as IR, NMR, DMA, TEM and physical testing methods. Adhesives used in food packaging are specially formulated by blending polymers together. Typical multilayer films in food packaging will combine structural layers such as ethylene polymers to oxygen barrier layers such as nylon or ethylene vinyl alcohol. An adhesive will generally contain a base resin similar to the polyolefin structural layer it will bond to, and functionalized polymer compatible with the base polymer. An example of a functionalized polymer is a maleic anhydride grafted polyolefin, which reacts with nylon or ethylene vinyl alcohol. Frequently, the adhesive is further formulated with a hydrocarbon rubber to improve its mechanical properties for high peel strengths.

ADH-1 was analyzed by IR and NMR to be a butene-based polyethylene containing 0.05% maleic anhydride. The level of butene is high, indicating a VLDPE. The thermal fractionation of ADH-1, shown in Fig. 4, reveals that no LLDPE is present. The ethylene sequence comes from two sources: the long sequence in HDPE ($T_m = 128^\circ\text{C}$) and the short in ethylene-co-butene-1 VLDPE ($T_m = 87, 78, 69, 60, 50^\circ\text{C}$ and lower). The long sequences corresponding to CH_2 lengths are 304 and 180, which are shorter

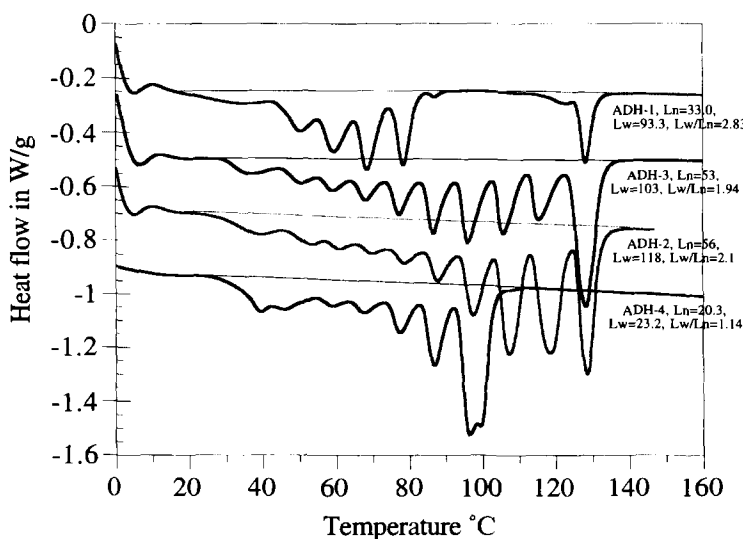


Fig. 4. Thermal fractionated adhesives.

than that of a typical HDPE sequence; we believe that this is due to the attachment of the maleic anhydride groups. The averaged sequences in the VLDPE are estimated to be 43, 35, 30, 26, 22 and shorter. The numerical expressions of \overline{L}_n , \overline{L}_w and $\overline{L}_w/\overline{L}_n$ measured in the ethylene repeating units are 33.0, 93.3 and 2.83. The crystallinity of the blend is low at 15.4%.

ADH-2 is an octene-based copolymer with ethylene propylene rubber containing 0.37 wt% maleic anhydride, as indicated by IR and NMR results. The fraction profile shows that it is a conventional octene-based ethylene copolymer with a broad comonomer distribution. The major ethylene sequences range from $(\text{CH}_2)_{320}$ to $(\text{CH}_2)_{18}$. The \overline{L}_n , \overline{L}_w , and $\overline{L}_w/\overline{L}_n$ measured in the ethylene repeating units are 56, 118, 2.1, respectively. The grafting is probably on EPR. The total crystallinity is 35%. Similarly, ADH-3, an octene copolymer grafted with maleic anhydride has 28.8% total crystallinity. The \overline{L}_n , \overline{L}_w , and $\overline{L}_w/\overline{L}_n$ are 53, 103, 1.94, respectively.

ADH-4 is a blend of ethylene vinyl acetate copolymer (EVA) and EPR as indicated from IR and NMR results. The thermal fractionation profile of ADH-4 shows that it may be the mixture of the two EVAs due to the unusual two very close, yet discrete, groups of ethylene sequence runs at $(\text{CH}_2)_{54}$ and $(\text{CH}_2)_{60}$. The fact that the slightly larger population of lower melting $(\text{CH}_2)_{20}$ and $(\text{CH}_2)_{18}$ fractions and a lower total crystallinity than that expected for typical fraction profiles of EVAs indicate the presence of an ethylene propylene rubber. The lower crystallinity is due to the weight contribution from rubber. The ethylene length distribution expressions of \overline{L}_n , \overline{L}_w , and $\overline{L}_w/\overline{L}_n$ are 20.3, 23.2, 1.14, respectively.

3.5. Maleic anhydride grafting

The grafting of maleic anhydride onto a nonpolar polymer allows it to react with a variety of polar groups and makes the grafted polymer a compatibilizer in blends. The free radical reactivity for peroxide-initiated grafting should be $3^\circ > 2^\circ > 1^\circ$. The 3° radical is a branch point; the 2° radical is part of the ethylene sequence; the 1° radical is the chain end. Grafting onto a tertiary position will not change the ethylene sequence, since the graft point is already a branch point. Similarly, grafting onto the chain ends does not alter the existing crystallizable ethylene sequence distribution. However, grafting onto a secondary position would shorten the ethylene sequence by introducing a new branch point. In Fig. 5, we compare thermal fractionation profiles of Flexomer 1085 before and after grafting. The grafted polymer (top curve) shows that the melting fractions of C254, C123, C82, C56 sequence lengths are lowered or reduced from the melting fractions of the ungrafted polymer (bottom curve) of C318, C146, C80, C56 fractions. The total crystallinity is decreased from 28.6% to 15.2%; however, the ethylene length distribution of \overline{L}_n , \overline{L}_w and $\overline{L}_w/\overline{L}_n$ are very similar (36–38, 67 and 1.77–1.88).

Another example of changes in fractionation profile of the base polymer with grafting of maleic anhydride is shown for HDPE in Fig. 6. HDPE base polymer and HDPE-g-MAN grafted at 2 levels (0.9% and 1.54%) were thermal fractionated from 135°C to 100°C in 5°C decrements. The profiles show that with HDPE grafting, larger

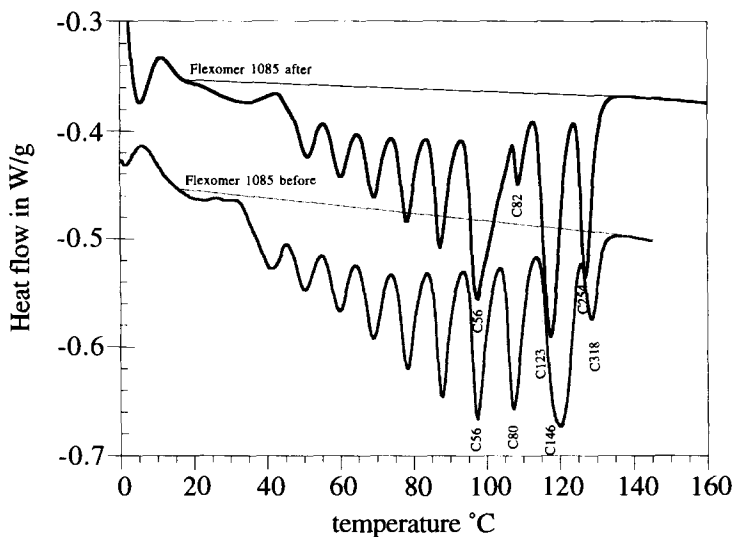


Fig. 5. A change of sequence length distribution of Flexomer 1085 before and after maleic anhydride grafting.

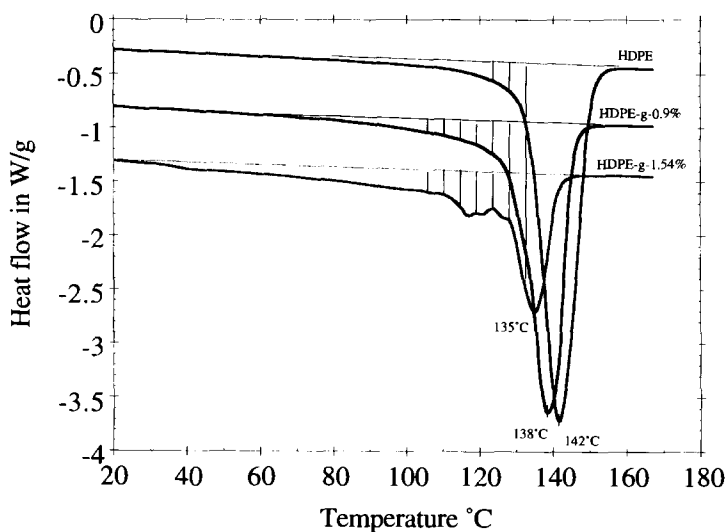


Fig. 6. A change of ethylene length distribution of HDPE before and after maleic anhydride grafting at two levels.

fractions of the crystallites melting below 130°C appear. Furthermore, the major melting peak of HDPE is reduced from 142°C for the ungrafted to 138°C at 0.9% maleic anhydride graft and 135°C at 1.54% graft. Both observations are consistent with the anhydride grafting onto the backbone of HDPE and interrupting the long ethylene

sequences. The repeatability of the fractionation profiles of the HDPE-g-MANs are not as good as those for the copolymers. This indicates that the grafting process is random and varies from pellet to pellet.

References

- [1] L. Wild, T.R. Ryle, D.C. Knobloch and I.R. Peat, *J. Polym. Sci., Polym. Phys. Edn.*, 20 (1982) 441.
- [2] L. Wild, *Adv. Polym. Sci.* 98 (1991) 1.
- [3] G. Glockner, *J. Appl. Polym. Sci., Appl. Polym. Symp.* 45 (1990) 1.
- [4] J.G. Bonner, C.J. Frye, G. Capaccio, *Polymer*, 34(16) (1993) 3532–34.
- [5] V.B.F. Mathot, M.F.J. Pijpers, *J. Appl. Polym. Sci.*, 39 (1990) 979–94.
- [6] R.A.C. Deblieck, V.B.F. Mathot, *J. Mater. Sci. Lett.* 7 (1988) 1276–80.
- [7] J.A. Parker, D.C. Bassett, R.H. Olley, P. Jaaskelainen, *Polymer* 35 (1994) 4140.
- [8] S.Y. Lai, G.W. Knight, *Annu. Tech. Conf., SPE*, 50th(2) (1992) 2084–7.
- [9] T.K. Vuong, P. Hedvig, *Proc. Tihany Symp. Radiat. Chem.* 6th(2) (1987) 463–9.
- [10] G. Attalla, F. Bertinotti, *J. Appl. Polym. Sci.*, 28(11) (1983) 3503–11.
- [11] M.Y. Keating, E.F. McCord, *Thermochim. Acta*, 243 (1994) 129–45.
- [12] J.D. Hoffman, J.I. Lauritzen Jr, *J. Res. Nat. Bur. Std.* 65A(4) (1961) 297–336.
- [13] S. Cheng, private communication.
- [14] F. Kopak, private communication.